Intra-Event Trends in Stable Isotopes: Exploring Midlatitude Precipitation Using a Vertically Pointing Micro Rain Radar

CATHERINE L. MULLER

School of Geography, Earth and Environmental Sciences, University of Birmingham, Edgbaston, Birmingham, United Kingdom

ANDY BAKER

Connected Waters Initiative Research Centre, University of New South Wales Australia, Sydney, New South Wales, Australia

IAN J. FAIRCHILD

School of Geography, Earth and Environmental Sciences, University of Birmingham, Edgbaston, Birmingham, United Kingdom

CHRIS KIDD

Earth System Science Interdisciplinary Center, University of Maryland, College Park, College Park, and NASA Goddard Space Flight Center, Greenbelt, Maryland

IAN BOOMER

School of Geography, Earth and Environmental Sciences, University of Birmingham, Edgbaston, Birmingham, United Kingdom

(Manuscript received 20 February 2014, in final form 9 September 2014)

ABSTRACT

Annual, monthly, and daily analyses of stable isotopes in precipitation are commonly made worldwide, yet only a few studies have explored the variations occurring on short time scales within individual precipitation events, particularly at midlatitude locations. This study examines hydrogen isotope data from sequential, intra-event samples from 16 precipitation events during different seasons and a range of synoptic conditions over an 18-month period in Birmingham, United Kingdom. Precipitation events were observed simultaneously using a vertically pointing micro rain radar (MRR), which, for the first time at a midlatitude location, allowed high-resolution examination of the microphysical characteristics (e.g., rain rate, fall velocity, and drop size distributions) that may influence the local isotopic composition of rainwater. The range in the hydrogen isotope ratio (δD, where D refers to deuterium) in 242 samples during 16 events was from $-87.0‰$ to $+9.2‰$, while the largest variation observed in a single event was $55.4‰$. In contrast to previous work, the results indicate that some midlatitude precipitation events do indeed show significant intra-event trends that are strongly influenced by precipitation processes and parameters such as rain rate, melting-level height, and droplet sizes. Inverse relationships between rain rate and isotopic composition are observed, representing an example of a local type of "amount effect," a still poorly understood process occurring at different scales. For these particular events, the mean δ value may therefore not provide all the relevant information. This work has significance for the testing and development of isotope-enabled cloud-resolving models and land surface models at higher resolutions, and it provides improved insights into a range of environmental processes that are influenced by subsampled precipitation events.

1. Introduction

Stable isotope ratios of rainwater are controlled by the origin of the water vapor, evaporation process at the source region, the rain-out history of the air mass,

Corresponding author address: Andy Baker, Connected Waters Initiative Research Centre, UNSW Australia, Sydney NSW 2052, Australia.
E-mail: a.baker@unsw.edu.au

DOI: 10.1175/JHM-D-14-0038.1

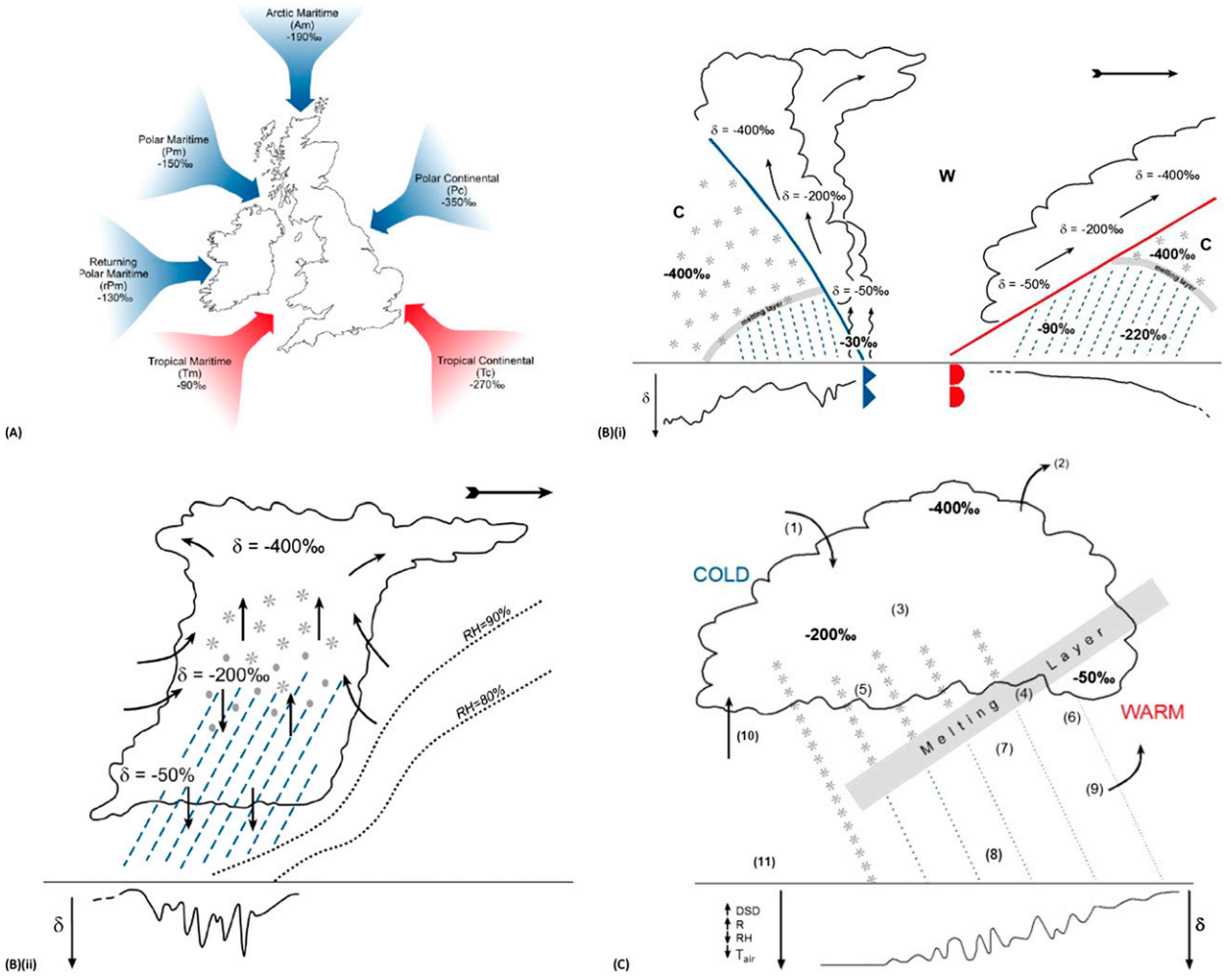

FIG. 1. Schematic diagrams showing the various influences on precipitation isotopic composition and fractionation processes at different scales, with theoretical δD values based on available literature. (a) Regional–synoptic [based on Hoefs (1997) and Coplen et al. (2000)] airmass type. (b) Mesoscale [based on Gedzelman and Lawrence (1990) and redrawn from Sodemann (2006), with changes] (i) stratiform/frontal and (ii) convective (graphs below schematics show isotope variability through event). (c) Microphysical [based on Miyake et al. (1968) and Sodemann (2006)]: 1) entrainment of air; 2) dissipation of dry air with isotopically depleted moisture at top of cloud; 3) formation of depleted ice crystals at low temperatures and diffusion of isotopic vapor to solid ice particles; 4) phase change; 5) kinetic isotope effects during snow formation; 6) removal of precipitation at cloud base; 7) equilibrium of droplets and vapor, dependent on drop sizes and RH; 8) isotopic exchange; 9) re-evaporation in layers of low RH (enrichment of rainfall at surface and depleted water vapor fed back into condensation process); 10) fast advective upward transport; and 11) below-cloud factors (T, RH, DSD, and R variability). Graphs below the schematic show decreasing isotope ratios and corresponding T, RH, DSD, and R trends.

atmospheric transport patterns, conditions leading to rain development, and phase and compositional changes that occur as the raindrops fall through and below the cloud (Celle-Jeanton et al. 2004; Fig. 1). The isotopic composition thus offers constraints on changes in the microphysical characteristics of the precipitating system, and there is a growing appreciation that patterns of behavior on shorter time scales offer new insights into the responsible mechanisms (Treble et al. 2005; Fairchild and Baker 2012). This has relevance for a range of environmental processes, particularly in situations where events may be subsampled. For example, there is relevance to understanding the isotopic composition of vadose and groundwater in zones that are recharged only by parts of precipitation events (Poage and Chamberlain 2001). It is also of interest to hydrometeorologists for cloud physics (e.g., Jouzel 1986), atmospheric water vapor transport (e.g., Risi et al. 2008a), and modeling microphysical and atmospheric processes, particularly GCMs and regional-scale land surface models, which increasingly have been isotope enabled to better understand model performance as well as to model and predict atmospheric isotopic

composition (Risi et al. 2012, 2013; Guglielmo et al. 2013). Furthermore, in contrast to tropical rainfall, the multiscale influences on the isotopic composition of midlatitude precipitation do not lend themselves well to univariate regression analysis because different processes can dominate the isotope signature at different spatiotemporal scales; for example, the air mass may have an opposing influence compared to within-event and life cycle effects (Berkelhammer et al. 2012; Sturm et al. 2010). This has resulted in difficulties in calibrating isotopic records. Studies of individual events therefore provide the most detailed information for partitioning controls and building up an understanding of variability.

Isotopic fractionation occurs during phase transformations when changes in the relative abundance of isotopes due to their differences in mass arise. There are two categories of isotope effects: equilibrium (e.g., condensation within clouds) and kinetic or nonequilibrium fractionation (e.g., evaporation, isotopic exchange with surrounding vapor, and re-evaporation of falling drops; Dansgaard 1964; Miyake et al. 1968). These fractionation processes influence the isotopic composition of precipitation, which is expressed as delta value δ (permil; ‰), the parts per thousand difference from a standard:

$$\delta = 1000\left(\frac{R_{\text{sample}}}{R_{\text{standard}}} - 1\right).$$

Isotopic composition of atmospheric water is initially controlled by ocean isotopic composition, sea surface temperature T_{air}, relative humidity (RH) of the atmosphere, and wind regime. Vapor found near the earth's surface is a mixture of newly evaporated surface water and lighter vapor from above that has been involved in fractionation/precipitation processes (Dansgaard 1964; Smith 1992; Lai et al. 2006; Strong et al. 2007). Condensation causes the isotopic depletion of the water vapor since heavy water molecules, $^{1}H^{2}HO$ and $H_2^{18}O$ [where ^{2}H can also be written as deuterium (D)], are converted preferentially into water droplets or ice crystals (which are therefore isotopically heavy). The aforementioned meteorological signals on precipitation isotopes are buffered by the effects of re-evaporation, isotope exchange between falling raindrops and water vapor, and equilibration with the surrounding vapor (Celle-Jeanton et al. 2004). Precipitation therefore has heavier δD and δ^{18}O values (henceforth denoted δ when referring to both isotopes) when it reaches the ground compared to when it was formed within the cloud (Gedzelman and Lawrence 1990). Thus, evaporation and isotopic exchange processes are very important processes involved as the raindrop falls below the cloud base (Lee and Fung 2008).

There are numerous environmental parameters (effects) that covary with the composition of precipitation: temperature, latitude, season, continentality, altitude, and precipitation amount (Dansgaard 1964; Yurtsever and Gat 1981; Rozanski et al. 1993). The first five of these effects are essentially all related to progressive fractionation during the cooling of an air mass and progressive removal of the condensate and are well understood, whereas the "amount effect" is polygenetic (Fairchild and Baker 2012); it is seen on different time scales and may have different origins. As a result, the underlying physical processes are still poorly understood and quantified (Risi et al. 2008a). The amount effect describes the negative correlation between the amount of precipitation at the surface and the proportion of heavy isotopes, which is physically related to low equilibration due to high below-cloud relative humidity and large droplets, decreased time for equilibration due to downdrafts, and the recycling of precipitation (Lawrence et al. 1982; Sodemann 2006). This effect has been observed and documented at monthly, intraseasonal, and annual time scales by numerous studies (e.g., Dansgaard 1964; Lee and Fung 2008; Risi et al. 2008a; Baldini et al. 2008, 2010; Field 2010; Kurita 2013) but has also been observed at shorter time scales in tropical rainfall (e.g., Risi et al. 2008a). Although a negative correlation between rainfall amount and δ exists, it has been noted that precipitation intensity does not correlate as well with δ when explored at short time scales [e.g., daily means (Risi et al. 2008a; Kurita et al. 2009) and event means (Vimeux et al. 2005; Kurita et al. 2009)] or for continental stations (Dansgaard 1964). However, this relationship has not been explored in detail at subevent time scales to date.

Values of δ also vary with rain-bearing systems, which influence rainfall quantity, moisture source, storm trajectory, and rain-out history (Crawford et al. 2013; Figs. 1a,b). For example, isotope ratios have been found to be higher in convective than stratiform clouds (Gedzelman and Lawrence 1990) and are more sensitive to short periods of rapidly changing rainfall intensities in convective events (Barras and Simmonds 2009). The highest δ^{18}O values are found in warm sectors, while the lowest values are found in the coldest air, in deep clouds, resulting from progressive depletion of heavy isotopes by fractionation during condensation. Cyclones are associated with low δ values (Dansgaard 1964) because of the isotopic distillation efficiency of such systems since water condenses at a high altitude and therefore has a low isotopic value (Treble et al. 2005; Risi et al. 2008a). The more developed and intense cyclones have the lowest δ values, with rainfall having an increasingly lower δ value closer to the center of a low-pressure system (Lawrence et al. 1982; Gedzelman and Lawrence 1990).

In additional to the aforementioned global, regional, and mesoscale influences, there are numerous finescale, local, and microphysical processes occurring both within and below the cloud (Fig. 1c). These also influence the final composition of precipitation at the surface. These processes are rarely taken into consideration when analyzing data at longer time scales but are very important when interpreting event-based data. Furthermore, the degree of equilibration and re-evaporation is controlled by the height of the cloud base and melting level, the relative humidity of the atmosphere beneath the cloud (and thus re-evaporation), and the size of the raindrops—which in turn is related to rain rate R (and therefore, the amount effect).

Although annual, monthly, and daily analyses of stable isotopes in precipitation are commonly made worldwide, only a few studies have looked at the smaller, individual precipitation event scales in which isotope ratios can vary significantly over a short period of time. For example, earlier analyses of single rainfall events have revealed within-storm variations of 10‰–12‰ for δ^{18}O (Rindsberger et al. 1990), while other work conducted at shorter (e.g., 30 min) time resolutions have found variations in δD of between 7‰ [southeast Australia (Barras and Simmonds 2009)] and 58‰ [California (Coplen et al. 2008)] or more. For example, a recent higher-resolution study [Cairns, Australia (Munksgaard et al. 2012)] found variations of up to 95‰ within a single 4-h period, despite the general meteorological conditions remaining stable.

Analyses of isotopic variations within individual rainfall events allow assessment of the gradual or abrupt changes in the microphysical, local, meteorological, and synoptic parameters influencing rain formation (Celle-Jeanton et al. 2004). Past studies have reported that the isotopic value of rainwater can vary significantly throughout individual precipitation events. Intra-storm samples therefore reveal a link between the isotopic signature and storm type, track, structure, and evolution (Gedzelman and Lawrence 1990; Smith 1992; Gat et al. 2001), yet there are other competing factors including rainfall intensity, changes in air mass, altitude at which rain is produced, the type of precipitation, conditions below cloud, and processes such as evaporation and condensation.

A number of specific isotopic trends have previously been identified and reported in the literature (Table 1). Decreasing trends (e.g., Gedzelman and Lawrence 1990; Taupin and Gallaire 1998; Celle-Jeanton et al. 2004; Coplen et al. 2008; Pfahl et al. 2012) occur when the δ value of rainfall events is observed to decrease with time, particularly for cold fronts. Indeed, Coplen et al. (2008) documented a large decrease of 51‰ for δD over a period of just 1 h for an extratropical cyclone. Such trends have been attributed to the decreasing impact of isotopic exchange and local increases in cloud-top heights occurring within a dynamic system (Gedzelman and Lawrence 1990; Coplen et al. 2008). These trends often reach a stationary value toward the end of the event, and when this is observed it is referred to as an L-shaped trend (Adar et al. 1991), or a stationary trend if the isotope values are relatively continuous throughout the event. Adar et al. (1991) attributed the L-shaped trend to intense rain showers, where rainwater becomes gradually more depleted in heavy isotopes. Others, for example, Celle-Jeanton et al. (2004), postulated that the constant values are due to the steady state in the condensation–rain-out process attained by convection, while Miyake et al. (1968) attributed it to the constant and unchanging height at which the rain was formed for one particular event. Increasing trends have also been identified (e.g., Miyake et al. 1968; Gedzelman and Lawrence 1990; Taupin and Gallaire 1998; Celle-Jeanton et al. 2004), suggesting that heavier isotope content in precipitation can increase with time, particularly rainfall associated with a warm front (Miyake et al. 1968). Gedzelman and Lawrence (1990) also observed a brief increase in δ^{18}O in one storm when the deepest clouds moved away prior to a break in the precipitation.

It is also possible that the trends identified above are observed at various stages throughout an event (e.g., Munksgaard et al. 2012). For example, V-shaped trends (a decreasing then increasing trend) have been identified in a number of studies (e.g., Levin et al. 1980; Rindsberger et al. 1990; Celle-Jeanton et al. 2004). In these events, the rain initially has a heavy isotope content that has been suggested to be caused by production in low-altitude clouds that are subject to evaporation during descent (Dansgaard 1964). This rainfall-production altitude increases because of the ascent of warm, humid air rising over a cold front in the case of frontal precipitation or because of convection and inflow of new air in the case of convective precipitation. This causes a decrease in both heavy isotope content and in-cloud air temperature, which reflects the progressive adiabatic condensation of vapor obeying the Rayleigh process (Gonfiantini et al. 2001), with maximum depletion reached at the highest rain intensity, which usually corresponds to maximum cooling at the passage of a cold front or when a convection cell reaches top height. Several explanations have been put forward for the increase in heavy isotope content of the rainwater toward the end of one event, for example (Celle-Jeanton et al. 2004), exchange between the falling drops and the vapor near the ground, infusion of new air masses with lower effective rain-out moving behind the front, residual precipitation formed

TABLE 1. Examples of within-event trends identified in the literature (in order of publication).

Reference	Isotopic trend(s) identified	Location	Type of events	Range of isotope values observed	Events
Munksgaard et al. (2012)	• Various	Cairnes, Australia	Convective, stratiform	δ^{18}O: from +2.6‰ to −19.6‰; δD: from +13‰ to −140‰	9 over 15 days in 8-month period
Risi et al. (2008b)	• W shaped	Niamey, Niger (Sahelian region)	Squall line systems	δ^{18}O: from ~−1‰ to −8‰	4
Barras and Simmonds (2009)	• Weak *R* relationship • Decreasing • Increasing • V shaped • No distinct/ variable • Stationary	Southeast Australia	Mixed frontal, convective, stratiform	δ^{18}O: from ~0‰ to −12‰	6
Coplen et al. (2008) [Yoshimura et al. (2010) modeled the same event]	Various trends within the event: • Decreasing • Increasing • V shaped	California coast	Extratropical cyclone	δD: from −22‰ to −80‰	1 over 2 days, separated into 6 zones of distinct isotopic behavior
Celle-Jeanton et al. (2004)	• Decreasing • Increasing • L shaped • V shaped	Avignon, France	Convective, stratiform	δ^{18}O: from ~−1‰ to −22‰	12 over 2 years
Taupin and Gallaire (1998)	• Increasing • Decreasing • W shaped	Niamey, Niger (Sahelian region)	Convective	δ^{18}O: from ~0‰ to −6‰	5
Adar et al. (1991)	• L shaped • V shaped	Israel	—	—	—
Rindsberger et al. (1990)	• W shaped	Israel	Various	δ^{18}O: from ~+1‰ to −12‰	Several over 2 years
Gedzelman and Lawrence (1990)	• Increasing • Decreasing	North Carolina	Extratropical cyclones	δ^{18}O: from ~+2‰ to −24‰	2
Miyake et al. (1968)	• *R* relationship • Increasing • Stationary • Decreasing • No distinct/ variable	Four different locations in and around Tokyo	Stratiform, convective, snow showers	δ^{18}O: from ~−2‰ to −18‰	10

at a lower elevation, and lower-intensity precipitation at the end of an event. In addition, two V-shaped trends, or a W-shaped trend, have also been observed within an event during which there is a successive passage of fronts (e.g., Taupin and Gallaire 1998; Rindsberger et al. 1990).

Therefore, despite similar-source air masses, events can have very different isotopic compositions and intra-event trends can be somewhat variable, indicating microphysical, local, meteorological, and synoptic signatures. However, the precise controlling mechanisms are still less well known or often speculative; therefore, our current understanding of how individual precipitation events translate into a mean value and the influence of transport variability is still uncertain (Helsen et al. 2005). The competing effects of the various factors (e.g., rainfall intensity, changes in air mass, altitude at which rain is produced, the type of precipitation, conditions below cloud, and processes such as evaporation and condensation) upon isotopic composition means that it has been difficult to differentiate between those primarily influencing the isotopic content of precipitation on an event scale. However, these parameters may have a large impact on studies utilizing

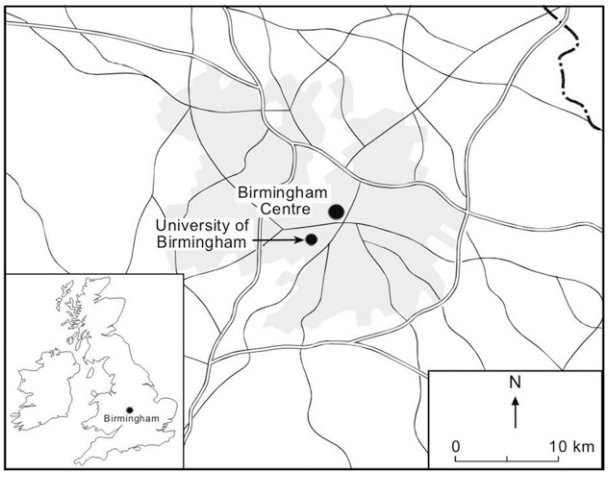

FIG. 2. Map of the location of Birmingham within the United Kingdom and the location of the sampling site within Birmingham.

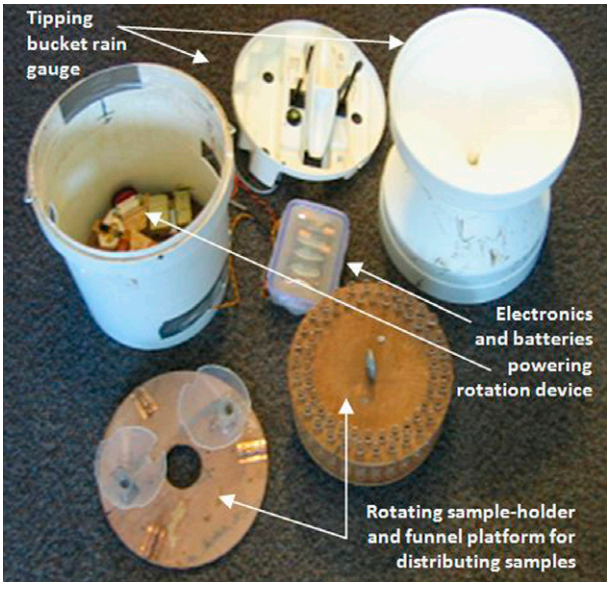

FIG. 3. Annotated photograph of low-cost bespoke automatic sampler.

stable water isotope records. Hence, understanding small-scale variability for individual precipitation events could be important if it reveals phenomena that are hidden by longer-term averaging, in the same way as previous research revealed processes hidden in monthly aggregated precipitation (e.g., Treble et al. 2005). A small number of studies have attempted this, yet few have used additional techniques in an attempt to interpret these within-event trends in isotopic variability.

This paper examines the intra-event trends in stable isotopes throughout a number of rainfall events using meteorological data and a vertically pointing micro rain radar (MRR) to explore these variations in more detail. MRRs are a relatively new method of measuring rainfall parameters at a specific location, providing microphysical information on R, drop size distributions (DSD), fall speed, and height of the melting layer [bright band (BB)]; the impact of these phenomena on isotopic composition have yet to be explored in detail. These measurements allow analysis of the variations in meteorological variables over very small temporal and vertical spatial scales. The main aim of this paper is to examine the extent to which hydrogen isotope ratios vary within individual events at a midlatitude location and to attempt to explain the reasons behind these variations.

2. Methodology

a. Sequential rainwater samples

Consecutive samples from 16 precipitation events were collected from an exposed location at the University of Birmingham (52°28′N, 1°56′W; 132 m above mean sea level; Fig. 2) between the beginning of April 2005 and October 2006. Samples were collected for a range of rainfall events, reflecting varying seasons, synoptic situations, and meteorological conditions. Initially (during the 2005 sampling campaign), a manual, amount-based sampling protocol was adopted, whereby a sterile, wide-mouthed bespoke Pyrex rain collector was used, from which 1-mL samples were collected and the time recorded. During the 2006 sampling campaign, however, a low-cost, semiautomated sequential precipitation collector was constructed, which involved using a 0.2-mm-resolution tipping-bucket rain gauge, which was modified to sequentially collect 10-mL samples for each tip of the internal bucket (Fig. 3). The sampling apparatus was exposed to the atmosphere just prior to the onset of precipitation and samples were collected as soon as the precipitation event ceased. Because humidity was close to 100% during the period that the sampling tube was open to the atmosphere (i.e., during the precipitation), evaporation will have been minimized. The samples were transferred to high-density polyethylene screw-top bottles, which were sealed immediately after sampling to prevent evaporation and stored at 4°C prior to isotope analyses.

b. Hydrogen isotope analysis

All samples were analyzed for hydrogen isotopes (D/H; δD). Analysis was carried out on a GV Instruments IsoPrime continuous-flow mass spectrometer at the University of Birmingham, using a EuroVector Elemental Analyzer preparation line. Approximately 0.3 μL of water was injected where reduction to

FIG. 4. Photograph of a vertically pointing MRR.

hydrogen took place at 1050°C over a chromium metal catalyst (Morrison et al. 2001). Each sample was repeated twice. Prior to the sample, two pulses of reference H_2 were injected to carry out a correction for H_3^+. Internal precision is 0.4‰, with external precision approximately 1‰. "Raw" reported values for the samples are corrected for instrumental drift through the run. Subsequently, standardization was carried out by calibration against laboratory and International Atomic Energy Agency (IAEA) reference standards. Values are expressed using the δ convention, relative to the standard [Vienna Standard Mean Ocean Water (VSMOW)].

c. Micro rain radars

Vertically pointing MRRs (Fig. 4) are small, portable, and easy to operate, and they provide a novel method of measuring rainfall that allows a more precise rain rate to be determined (Diederich et al. 2004; Muller et al. 2010). MRRs are frequency modulated continuous wave (FMCW) Doppler radars operating at 24 GHz; the frequency deviation (Doppler frequency) between the transmitted and the received signal is a measure of the falling velocity of the rain drops. They measure the backscatter of radiation from precipitation-sized particles in 30 range bins that, in this study, allow measurements between the surface and 3000 m. Information on a number of microphysical parameters are generated every 60 s, including the fall velocity, DSD (drop sizes between 0.1 and 4.5 mm), liquid water content (LWC), and *R*. MRRs allow the processes influencing isotopic variability to be assessed, such as identification of the melting layer (bright band) and exploration of the amount effect on within-event isotopic variability, since they provide high-temporal-resolution data over a range of vertical heights. MRRs provide high-temporal-resolution information on the characteristics of the precipitation every 100 m from the ground up to 3000 m but were only available during the 2006 campaign. During the 2005 campaign, rainfall data were obtained from a local tipping-bucket rain gauge.

d. Other supporting data

Following the methodology of Muller et al. (2008), the Hybrid Single-Particle Lagrangian Integrated Trajectory model, version 4 (HYSPLIT4; Draxler and Rolph 2003), was used to calculate backward trajectories from Birmingham at 6-hourly intervals up to a period of 5 days at 500, 1000, and 1500 m above ground level. These back trajectories were used as supporting information for assessing source areas and airmass type, important factors influencing the isotopic composition of precipitation in midlatitude locations. A range of in situ meteorological data from the university's weather station adjacent to the sampling site and archived synoptic charts (from www.wetterzentrale.de) were also used to assist with analyses and interpretation of within-event trends.

3. Results and discussion

a. Event averages

Table 2 summarizes the overall conditions and mean isotope values from the individual events. When exploring the event-averaged data, there were no obvious, consistent, or significant relationships with rain rate, airmass type (little variability evident in back trajectories), wind direction, or precipitation type. It is expected that this is because of competing local, finescale, or microphysical factors that are having a greater influence on the resulting mean isotopic composition than larger-scale factors. This is explored in detail in the subsequent sections.

b. Intra-event trends

The δD of samples from a small number of precipitation events remains fairly consistent throughout, varying by as little as 3.9‰, indicating that either larger-scale

TABLE 2. Table summarizing overall conditions and mean isotope values from the individual events. Tc is tropical continental, rPm is returning polar maritime, Tm is tropical maritime, and Pm is polar maritime.

Date	Sampling method	No. of samples	Start time (UTC)	Duration h	Duration min	Mean R from MRR (mm hr^{-1})	Max δD (‰)	Min δD (‰)	Mean δD (‰)	Range of δD (‰)	Type of precipitation	Wind direction	Source area	Airmass type	Isotopic trend?
26 Apr 2005*	Manual**	40	1250	1	00	—	−20.2	−54.4	−39.8	34.2	Occlusion	SW	Continental	Tc	Increasing then two V shaped (W shaped)
24 May 2005*	Manual**	17	0843	0	29	—	−12.4	−18.3	−15.6	5.9	Cold front	S	Maritime	rPm	No distinct/ variable
15 Jun 2005*	Manual**	4	1105	0	45	—	−25.7	−29.6	−28.2	3.9	Frontal system with convection	S	Maritime	rPm	Increasing
24 Jun 2005*	Manual**	18	0908	0	37	—	−26.0	−41.9	−34.7	15.9	Convective showers	N	Maritime	Tm	Increasing
5 Jul 2005*	Manual**	17	1225	0	44	—	−14.2	−35.9	−28.2	21.7	Convective showers	NW	Maritime	Tm	Inverted V shape
28 Jul 2005*	Manual**	8	1004	0	44	—	−14.4	−24.9	−21.2	10.6	Postfrontal convection	E	Maritime	Pm	V shaped
12 Jun 2006	Automatic	8	1339	0	19	11.53	−10.0	−28.9	−23.3	18.9	Convective showers	S	Continental	Tc	V shaped; R relationship
13 Jun 2006	Automatic	14	1330	2	40	3.88	−7.7	−23.7	−15.5	16.1	Convective showers	W	Maritime	Tm	No distinct/ variable
20 Jun 2006	Automatic	6	1827	1	44	0.48	−6.2	−17.3	−13.1	11.1	Cold front	NW	Maritime	rPm	Increasing
22 Jul 2006	Automatic	22	1424	2	6	2.26	+9.2	−21.5	−7.2	30.7	Convective showers	NE	Maritime	Tm	Decreasing
29 Sep 2006	Automatic	8	1614	0	36	0.98	−21.9	−52.8	−45.4	30.8	Cold front with convection	S	Maritime	Tm	Increasing
5 Oct 2006a	Automatic	18	0752	3	16	0.63	−31.6	−87.0	−61.6	55.4	Warm front/ occlusion	S	Maritime	rPm	Increasing
5 Oct 2006b	Automatic	12	1415	2	5	3.08	−21.2	−30.3	−26.6	9.2	Cold front and orographic enhancement	S	Maritime	rPm	V shaped; R relationship
6 Oct 2006	Automatic	28	0000	11	0	2.58	−2.9	−25.9	−10.9	23.0	Cold front with convection	SW	Maritime	rPm	General decreasing; R relationship
9 Oct 2006	Automatic	6	0937	0	37	2.03	−21.8	−32.2	−27.0	10.4	Cold front with convection	S	Maritime	rPm	Decreasing
11 Oct 2006	Automatic	16	1440	2	45	1.94	−30.7	−70.0	−60.3	39.5	Convective showers	S	Continental	Tc	V shaped; R relationship

* MRR not in use for these events.

** Entire event not sampled.

processes were dominating or that local conditions were fairly stable. However, for the majority of events, the δD value from within-event samples varied significantly, by as much as 55.4‰ (in one event lasting just over 2 h). Even in one extreme convective event (12 June 2006) that lasted less than 20 min, δD varied by as much as 18.9‰ (Table 2). For these particular events, the knowledge of small temporal variations in isotopic composition is likely to be most significant since mean δD values only provide limited information about the precipitation event. Birmingham is a midlatitude, inland city that experiences a range of air masses, so a larger range of δD values may be expected (e.g., Munksgaard et al. 2012). Nevertheless, given the predominant influence of maritime air masses, this large range is perhaps unexpected within a single rainfall event, especially for events where the source air mass remains stable. Thus, more localized or microphysical fractionation processes are likely to be operating.

As discussed below, a number of the sampled events display distinct, fluctuating isotopic trends throughout; Fig. 5 shows schematic diagrams of the various intra-event trends identified, summarizing the main features and associated phenomenon as well as the below-cloud, local conditions (e.g., air temperature T_{air}, RH, and DSD) that play a significant part in the resulting intra-event isotopic composition of the precipitation.

The event on 26 April 2005 (Fig. 6) displayed an increasing trend at the beginning of the event prior to the break in precipitation (rising from −26‰ to −20‰), followed by two small V-shaped trends (corresponding to light isotope peaks of 54.4‰ at 1355 UTC and −49.7% at 1405 UTC, separated by a slight increase to −43.7‰), that is, a W-trend is evident (Celle-Jeanton et al. 2004; Rindsberger et al. 1990). There appears to be a relationship with R throughout this event as low R occurs at the start of the event, corresponding to isotopically heavy samples, and an increase in R is observed to correspond with isotopically light samples toward the second part of the event; however, because of the lack of high-resolution MRR data, it is difficult to be certain about the strength of the relationship, particularly during the peak of the rainfall (during this time, R appeared to be stationary, but this is because of the coarse resolution of the rain gauge, which did not capture the high-intensity rainfall).

The T_{air} and RH data were only available at ground level; therefore, a complete understanding of conditions throughout the atmosphere cannot be fully deduced. Variability in these data, however, can provide some insights. Ground-level RH varied by 6% throughout the event, though this does not appear to explain much of the isotopic trend observed (i.e., lower RH may imply a higher evaporation), while T_{air} only varied <1°C throughout the event, so it is unlikely to have played a significant role, though it does display the expected positive relationship with δD. The variability is therefore likely to be linked to a range of controlling factors. For example, the isotopic enrichment occurring during the initial stages may be a result of equilibration with low-level vapor or rainfall production in warmer, low-level clouds or at the base of a cloud with a low condensation rate (though cloud base cannot be estimated from the MRR in this case). Indeed, since the first part of the sampling campaign collected rainfall from the end of the first frontal system rather than that initial rainfall (which was not captured) as the event was associated with a fragmented occluded front, the isotopic behavior may be explained by the residual precipitation forming at a lower elevation at the end of a front, which, as observed, is of lower intensity as the front dissipates (Celle-Jeanton et al. 2004), thus resulting in more enriched samples, albeit more depleted than the rain at the start of the event.

The second part of the event displayed two V-shaped trends (Celle-Jeanton et al. 2004; Levin et al. 1980), that is, a W trend (Rindsberger et al. 1990), of stable isotope compositions. It is likely that the altitude at which rain was produced increased throughout the event because of the frontal lifting of warm, humid air over the occluded front. Both heavy isotope content and ground-level T_{air} gradually decrease, reflecting the progressive adiabatic condensation of vapor obeying the Rayleigh process, with the maximum fractionation reached at the highest rain intensity—during the middle of the event—which usually corresponds to maximum cooling at the passage of a front (Gonfiantini et al. 2001). As air becomes increasingly saturated throughout an event, heavy isotope enrichment due to diffusion with surrounding vapor is reduced with time, resulting in lighter isotope signatures; however, the ground-level RH data do not reflect this for this event, suggesting rain intensity may have played a greater role. Slight enrichment in ^{2}H was observed during the final stages, which is likely to have been due to decreasing rainfall intensity (R–δD relationships are discussed further in section 3c).

The event on 5 July 2005 (Fig. 6) also displayed distinctive features. Rainwater was isotopically depleted in ^{2}H at the beginning, and δ values then increased for a time while the air was less saturated and precipitation intensity was low (and thus potentially more susceptible to evaporative exchange). Toward the end of the event, as the front progressed, the precipitation became more intense and the air saturated (increase in RH), the isotope values became lighter (Fig. 6). Since the MRRs were not available during the early 2005 sampling,

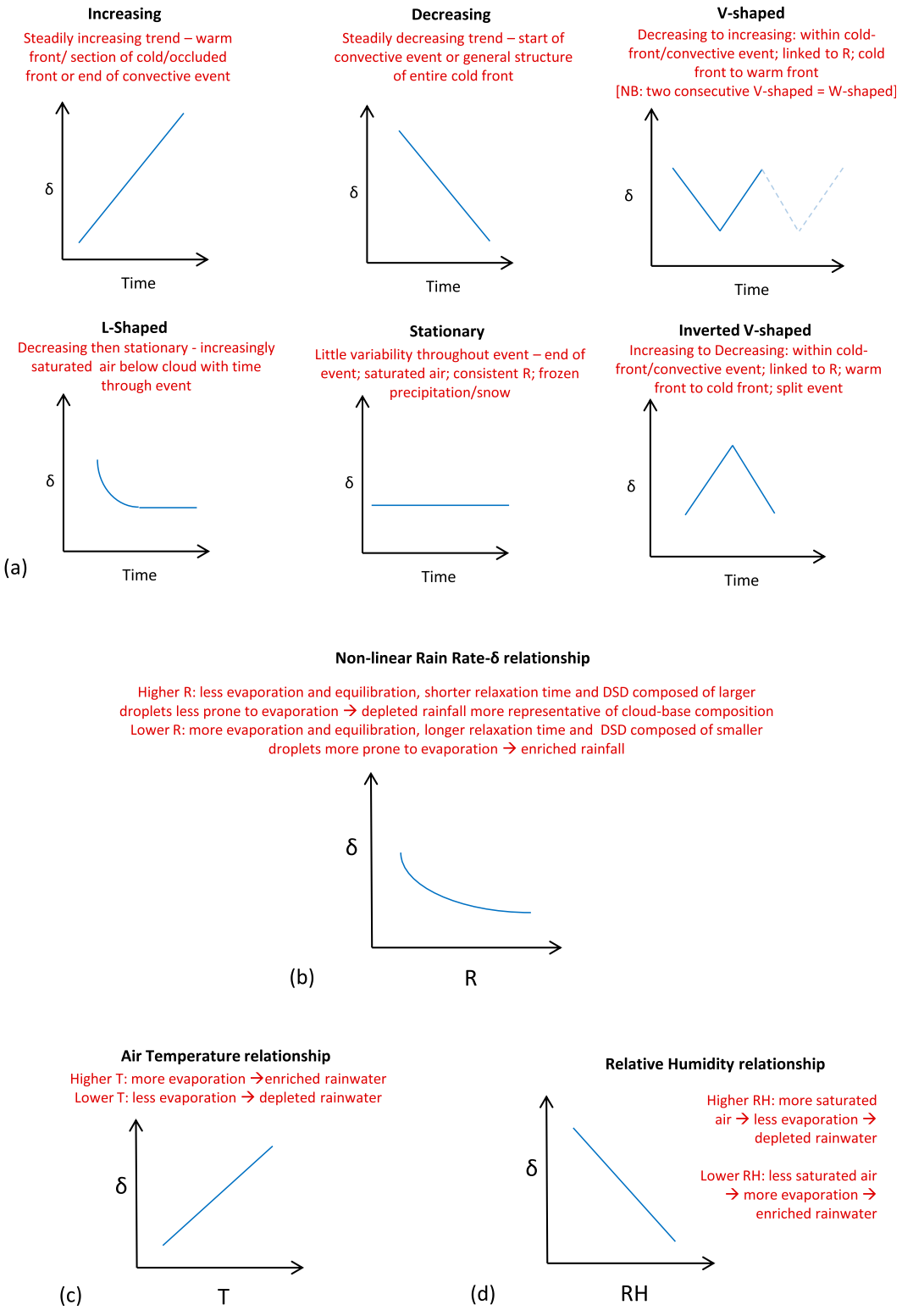

FIG. 5. Schematic diagram showing local (a) surface δ trends over time, (b) *R*–δ relationship, (c) T_{air}–δ relationship, and (d) RH–δ relationship.

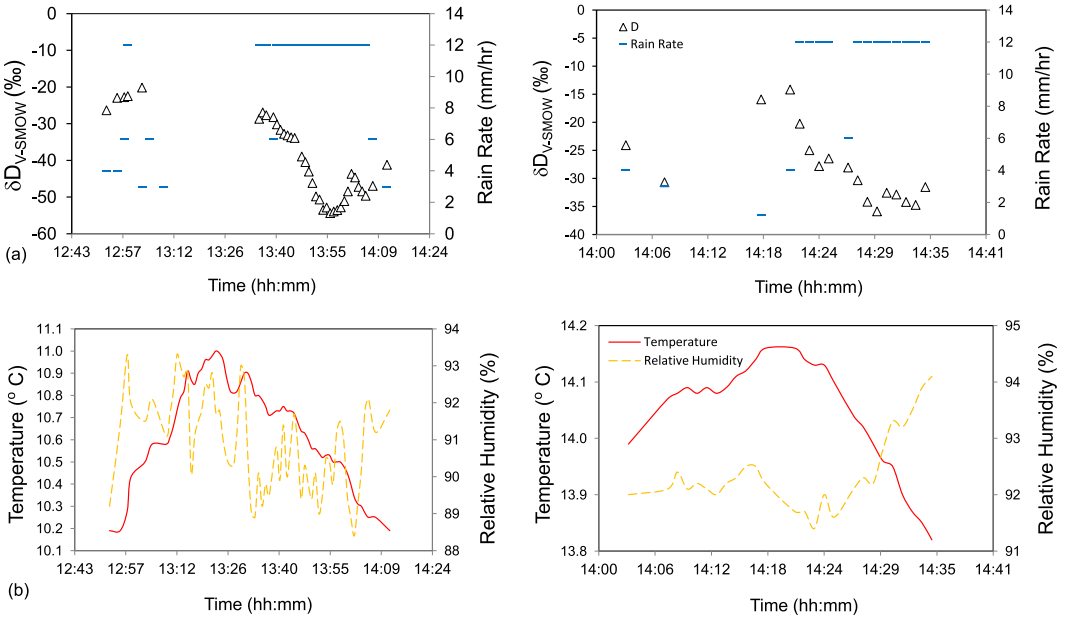

FIG. 6. Events showing W-shaped trends: (a) time series plots of R (derived from tipping-bucket rain gauge; mm h^{-1}) and δD; (b) time series of T_{air} and RH for (left) 26 Apr and (right) 5 Jul 2005. (Note that max observed R was limited by the resolution of the rain gauge used during this sampling campaign and does not indicate that the rainfall was stationary.)

however, rain intensity can only be postulated based on a local, coarse-resolution rain gauge data.

Increasing trends were evident within several events (Table 2), and two are discussed here (Fig. 7). First, on 29 September 2006 (Fig. 7), there was an initial period of high-intensity convective rainfall and high fall velocity during vertical descent that was associated with light δD values (minimum value $-52.8‰$) at the beginning of the event. Moist convection, acting primarily in the vertical dimension, is triggered by adiabatic, diabatic, or orographic processes in conditionally unstable air (Sodemann 2006). Rapid updrafts cause fast condensation and precipitation formation resulting in intense showers with large droplets. The lightest values during this event could therefore be associated with rainfall formed in deep clouds in the coldest parts of the system (Gedzelman and Lawrence 1990). However, it must be noted that the isotopic signature of convective precipitation is not as well understood as that of stratiform precipitation because of its complex nature; large drop sizes, higher intensities, and rapid transport in down drafts can, in fact, counteract equilibration (Sodemann 2006).

The precipitation event that was sampled on the morning of 5 October 2006 (Fig. 7) was associated with a warm front and occlusion and also displayed a steadily increasing isotopic trend, with the exception of the initial sample, which had a slightly elevated δD value, possibly due to evaporation in an initially less-saturated atmosphere. A large range of δD was observed, from very low values of $-87‰$ near the beginning to $-31.6‰$ at the end of the event. However, evaporation cannot explain this overall increase since RH varied only slightly within the event and increased overall; T_{air} did, however, increase by 1.5°C throughout the event, though this is unlikely to explain all increases in δD observed. When the MRR data for this event are explored, a low-lying BB is evident within the observation range of the MRR. The BB—or melting layer—is the region in the atmosphere where frozen particles melt into rain and produce a stronger radar reflection than the regions of frozen particles above and rain below; BBs are seen in MRR data as enhanced reflectivities in the vertical dimension and where fall velocity increases as frozen particles melt into rain droplets (melting layer). Figure 7c shows a sodargram of fall velocity during this event; although R was fairly low throughout this event, fall velocities during vertical descent of the droplets were quite high—something that could not be observed without the use of an MRR. The plot also shows that this melting layer increased in height throughout the event, resulting in an increase in the relaxation distance, which would have allowed more time for the droplets to equilibrate with the surrounding vapor, particularly important for larger droplets. Therefore, more enrichment of heavy isotopes via evaporation is likely to have occurred via these microphysical

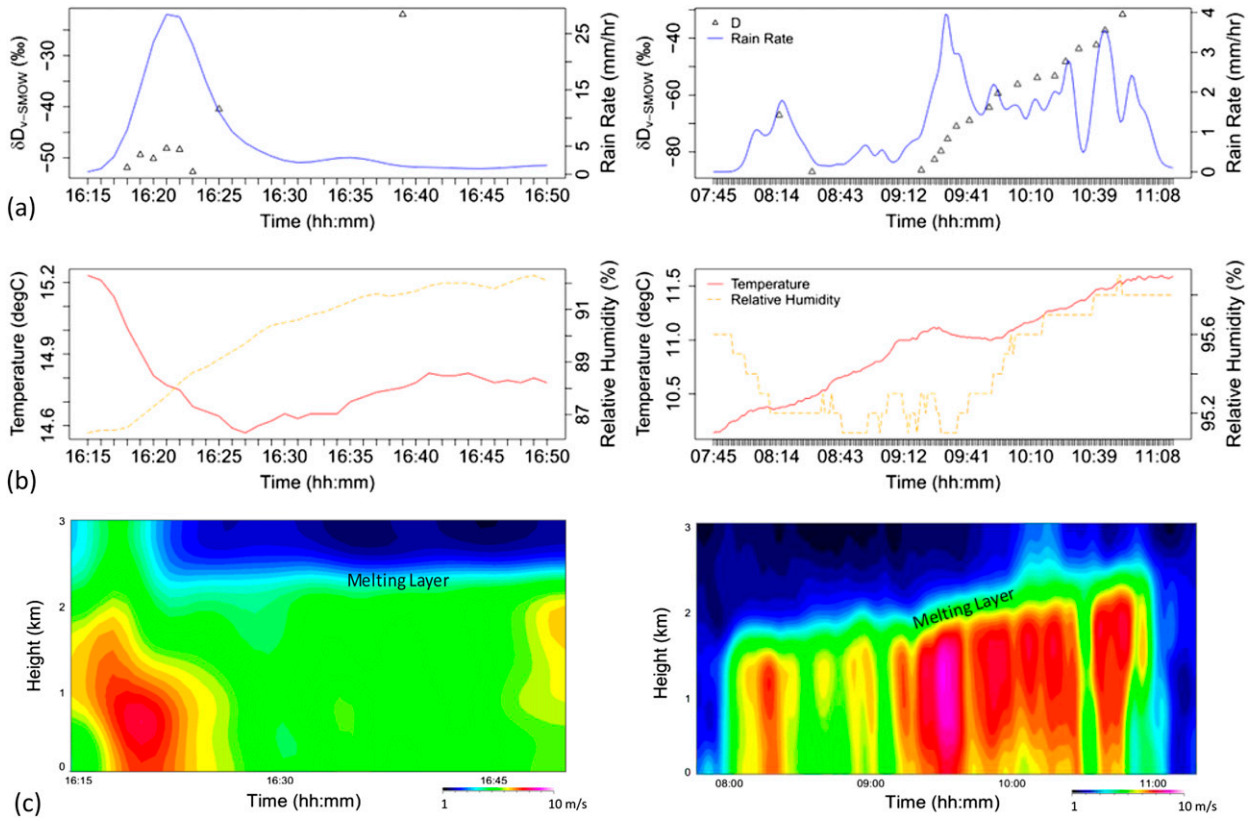

FIG. 7. Events showing increasing trends: (a) time series plots of minute-averaged R (mm h^{-1}) and δD, (b) time series of T_{air} and RH, (c) plot of fall velocity (m s^{-2}) with height for (left) 29 Sep and (right) 5 Oct 2006. (Melting layer annotated where visible.)

processes (this is explored further in section 3d). At a warm front, warm and moist air flows upward over colder, denser air masses. Large-scale condensation and fractionation occurs in these regions, and as a result, water vapor becomes increasingly depleted in heavy isotopes as it is lifted to higher, colder air. As this occurs, there is a gradual increase in the isotopic signature of surface precipitation toward the surface of a warm front due to the increasing rate of condensation altitudes (Gedzelman and Lawrence 1990). Dansgaard (1964) noted that the height of the front above the ground as well as the melting layer is important to the resulting isotopic composition of precipitation. Furthermore, Celle-Jeanton et al. (2004) proposed explanations for the increase in δD toward the end of an event, including residual precipitation forming at a lower elevation, lower rainfall intensity at the end of an event as the front dissipates, exchange processes, and inputs of new air masses. However, these explanations do not fully explain the reasons behind the increasing trend seen in the first event on 5 October 2006, since the precipitation clearly did not form at a lower elevation during the final stages and no change in air mass was evident during this event.

In contrast, decreasing isotopic trends (Fig. 8) were also observed. The event on 22 July 2005 (Fig. 8) was highly convective, with thunder and lightning noted; positive isotopic values—as seen at the beginning of this event—are often related to the proximity to source of the moisture, which for convective events can be more localized (Kurita 2013). High fall velocities were observed, particularly from approximately 1510 UTC onward, possibly indicating some evidence of a relationship with R because of the associated depletion in heavy isotopes. However, there was an overall decreasing trend in δD, with very heavy, positive isotope values at the beginning of the event. Therefore, both T_{air} and RH appear to have had an impact on δD throughout the event; warmer T_{air} (22°C) and lower RH (73%) at the start of the event may have resulted in more evaporation in the undersaturated air compared to the end of the event (T_{air} is 17°C, RH is 94%). Indeed, re-evaporation has the greatest impact during the initial stages of precipitation when the water vapor content of the air is lower; the effect reduces as relative humidity reaches saturation and isotopic equilibrium is established between vapor and rainwater (Celle-Jeanton et al. 2004). Re-evaporation generally

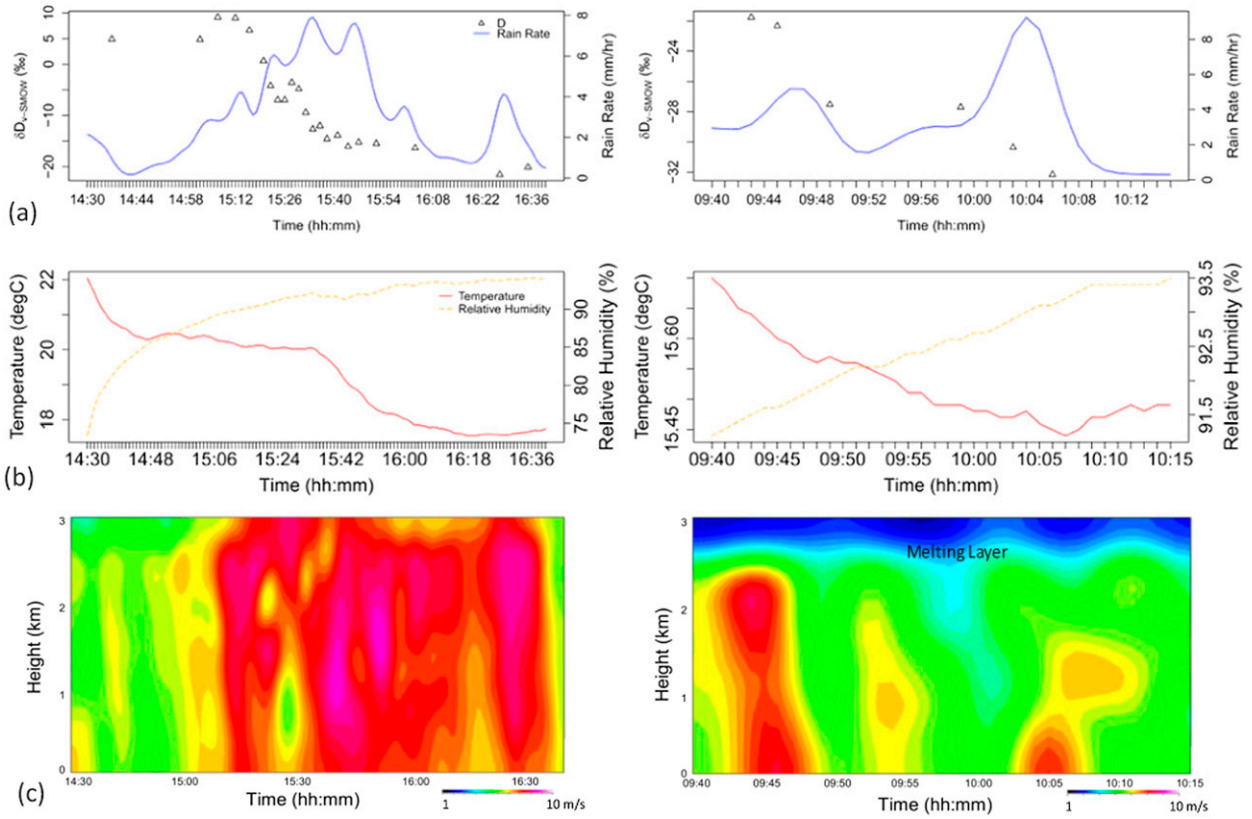

FIG. 8. Events showing decreasing trends: (a) time series plots of minute-averaged R (mm h^{-1}) and δD, (b) time series of T_{air} and RH, (c) plot of fall velocity (m s^{-2}) with height for (left) 22 Jul and (right) 9 Oct 2006. (Melting layer annotated where visible.)

increases the δD value of raindrops and decreases the δD value of the water vapor. Furthermore, for events showing a gradually decreasing and stabilizing trend (i.e., L-shaped trend), isotopic equilibrium between droplets and vapor is likely to have been reached (e.g., Adar et al. 1991; Celle-Jeanton et al. 2004; Barras and Simmonds 2009). This may explain the isotopic composition of the precipitation at the end of this event.

Another event displaying decreasing values, albeit a smaller range in values (10.4‰), was sampled on 9 October 2006 (Fig. 8). No clear overall relationship between R/vertical fall velocity and isotopic composition can be seen in this event (with the exception of the two samples collected during the peak rainfall intensity, but small sample size limits interpretation), and RH and T_{air} also showed some relationship with δD; however, variability was much smaller throughout this event. It is therefore likely that a stronger forcing was affecting the isotope values during this event, possibly because of the movement of the cold front, changes to the air mass, or in-cloud processes. Although analysis of the back trajectories during this event does not indicate a significant change in air mass, the small decrease in values may be a result of the passage of the cold front. A cold front often begins with a fluctuating isotopic signature, which then moves toward an increasingly depleted isotopic signature (Gedzelman and Lawrence 1990). Furthermore, convection associated with a cold front can lead to the occurrence of precipitation episodes with very low δ values, which may have contributed to the decrease in isotopic composition during the peak of the rainfall.

c. *Rain-rate relationships*

As previously highlighted, the amount effect is seen on different time scales, but broadly describes the inverse relationship between precipitation amount and the proportion of heavy isotopes. Since rainfall amount and R are inherently related, the relationship between R and isotope ratio was examined in order to explore a local rain intensity effect. Initially, the overall δD–R relationship was assessed for all individual samples grouped together. However, no significant relationship was found because of the nonlinear and variable relationship between R and isotopic composition, as well as other competing controls on the isotopic composition (e.g., life cycle stage, airmass type, rain-out history,

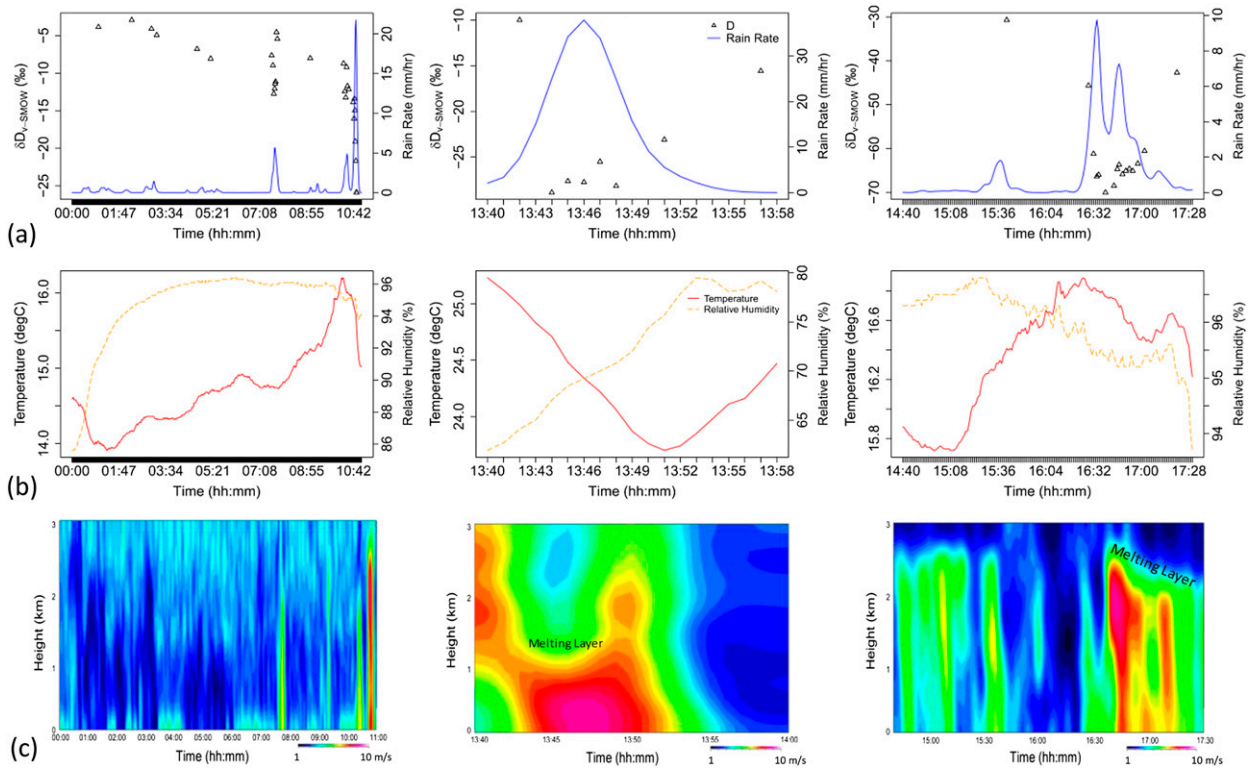

FIG. 9. Events showing rain-rate relationships: (a) time series plots of minute-averaged R (mm h^{-1}) and δD; (b) time series of T_{air} and RH; (c) plot of fall velocity (m s^{-2}) with height for (left) 6 Oct, (middle) 12 Jun, and (right) 11 Oct 2006. (Melting layer annotated where visible.)

and storm type) that occur for individual precipitation events.

However, exploring individual events in detail using MRR (and rain gauge) data has highlighted that short, subevent precipitation intensity variability can indeed have a strong influence on isotope ratios, with some events displaying a clear nonlinear, inverse relationship between δD and R (Fig. 5b). Events showing clear relationships between R and δD are shown in Fig. 9. On 6 October 2006, a cold-front event (with convective elements) lasting several hours was sampled. There is a significant nonlinear relationship with precipitation intensity throughout this event, particularly visible during the sharp peaks in rainfall. Initially, enriched values during the low-intensity precipitation are likely to be due to evaporation in a less-saturated atmosphere; variations in RH and T_{air} can therefore help explain some of the isotope variability but not the observed rapid fall in δD. The peaks seen in the MRR data showing fall speed with height clearly correspond to major dips in δD, supporting the notion that higher fall speeds result in depleted rainwater at the surface, expected to be linked to less time for evaporative exchange between the droplets and the surrounding vapor.

Another highly convective event on 12 June 2006 (Fig. 9) displayed a V-shaped trend with a large range of isotope values (39.5‰). This event also demonstrates the impact that increasing rainfall intensity—even over short time periods—can have on isotope ratios. Although low initial RH may have contributed to evaporative enrichment during the initial stage of the event, it cannot fully explain the variability throughout the event. An unusually low melting-level height in the middle of this event may have also contributed to the isotopic content of precipitation, suggesting that the depleted ground-level rainwater values are more similar to cloud droplets at cloud base at the peak of this event because of the short relaxation distance. The 11 October 2006 convective event (Fig. 9) also displayed a V-shaped trend; the isotopic ratio for this particular event appears to be dependent upon ground-level R and fall speed with height, while RH and T_{air} appear to have no overall influence, and although melting layer height decreased toward the end, it also does not appear to have had a major effect on δD.

Intense precipitation contains larger droplets with a lower surface area–volume ratio that fall more rapidly, therefore having less time to evaporate. Bolin (1958)

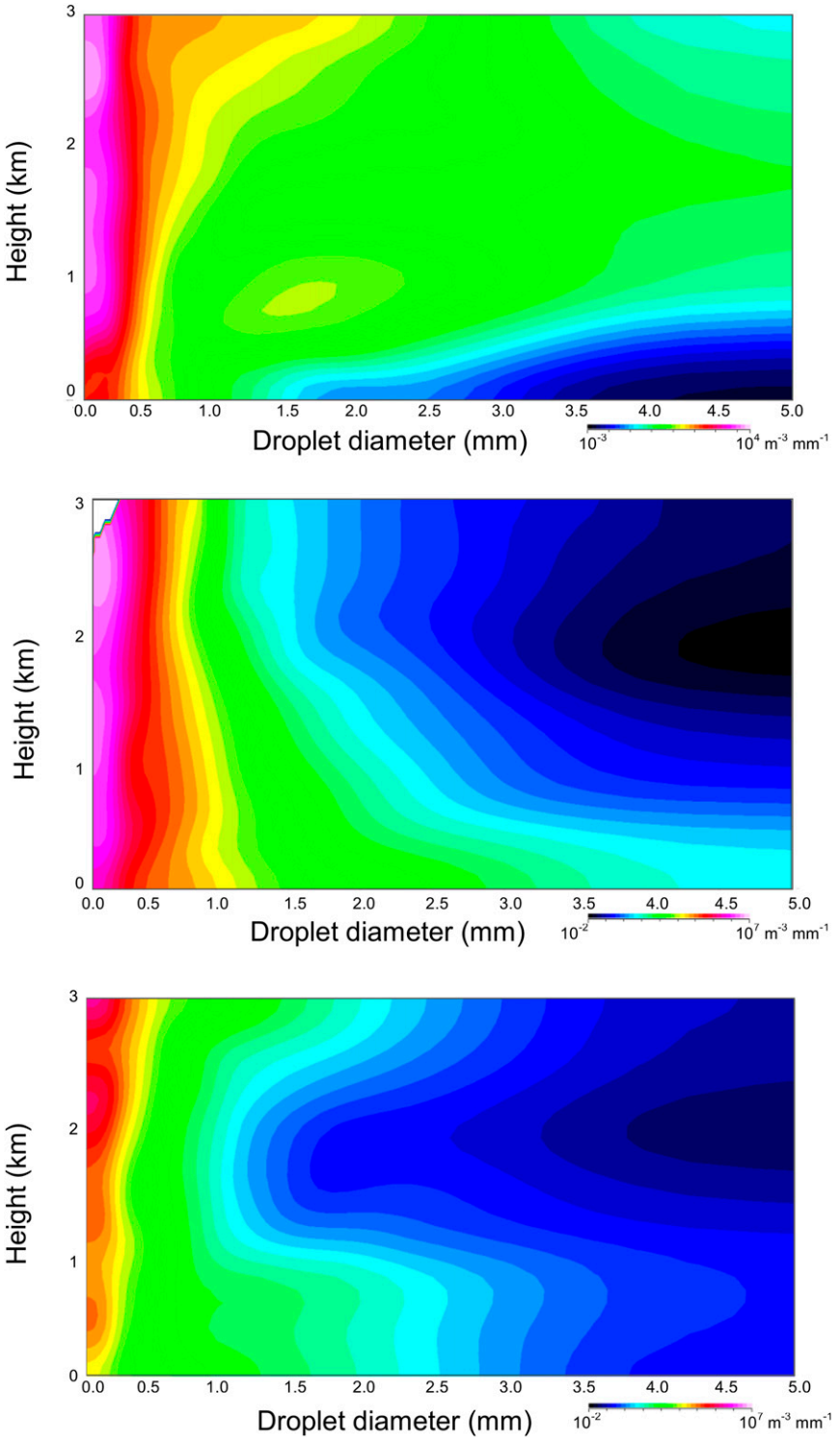

FIG. 10. Plots showing DSD with height for (top) initial, (middle) middle, and (bottom) final stages of the V-shaped convective event on 12 Jun 2006.

TABLE 3. Relaxation time and distance for the exchange process between falling water droplets and the ambient air moisture. [Using equations derived from Gat et al. (2001) (after Bolin 1958; Friedman et al. 1962; Houze 1993).]

Drop radius (cm) x	Relaxation distance (m) y	Relaxation time (s) y	Terminal velocity ($m\,s^{-1}$)
0.01	5.1	7.1	1
0.05	370	92.5	2
0.10	1600	246	3.5
Equation	$y = 172\,014x^2 - 1201.3x$	$y = 13\,118x^2 + 1152.8x$	

suggested that only strong showers greater than $10\,mm\,h^{-1}$ will represent the composition of precipitation at the cloud base up to 1000 m above the ground. For the 6 October and 12 June 2006 events, R reached intensities above the $10\,mm\,h^{-1}$ threshold (Bolin 1958); thus, these samples may provide some indication of cloud-base isotopic composition (e.g., from −15‰ to −25‰ on 6 October and from −22‰ to −29‰ on 12 June).

Large drop sizes, higher intensities, and rapid downdrafts from upper levels can therefore result in episodes of isotopically lighter precipitation during convective storms. Figure 10 shows the vertical DSD for the initial, middle, and final stages of the 12 June 2006 event (Fig. 9), which can be used to explore the changes that occurred within the event and as the precipitation fell through the atmosphere. There were a greater number of larger droplets in the upper levels (~3000 m) compared to near-ground-level precipitation during the light rainfall at the start of the event, providing some evidence for breakup but for mostly evaporation—because of the overall decrease in volume—during descent. During the most intense and isotopically lightest rainfall, there was a shift in the DSD; there was a greater proportion of larger droplets near the ground, as smaller- and medium-sized droplets from above coalesced during descent (Mason and Ramanadham 1954) and/or as larger droplets fell more rapidly to the ground. Evaporation has less of an effect on these larger droplets, which will therefore have an isotopic composition more similar to that within the cloud. Although large droplets only represent a small proportion of the overall droplets, these larger droplets play an important role in governing the isotopic composition of rainwater at ground level during intense rainfall (Gat et al. 2001; Bolin 1958; Friedman et al. 1962; Houze 1993). Furthermore, melting level was particularly low during this time. During the final stage of the event, the number of overall droplets—especially the smaller droplets—decreases toward ground level (Fig. 10), indicating that some evaporation may have occurred; however, there is also a decrease, followed by an increase in larger droplets between the upper levels and ground level, possibly indicating initial evaporation or breakup, followed by coalescence of smaller droplets at lower levels. The role of DSD and melting layer heights are investigated in more detail below.

d. Relaxation heights and DSD

Data on DSD and melting layer height can be used to explore the local rain intensity effect in more detail. As discussed, at $R < 10\,mm\,h^{-1}$, rainwater collected at ground level will essentially be a modified version of that found in the cloud (Bolin 1958). Depending upon the height of the melting level, R and thus the DSD, a proportion of the rain droplets will equilibrate below the melting level. The ''relaxation height'' or ''relaxation time'' (Gat et al. 2001) is the height needed, or time required, to achieve $1/e$ of the final equilibrium state, which for raindrops is dependent upon droplet size. Table 3 shows the theoretical relaxation time and distance for the exchange process between falling water droplets and the ambient air moisture (Gat et al. 2001; Bolin 1958; Friedman et al. 1962; Houze 1993).

The event on 5 October 2006 can be explored in detail, since the melting layer height varied within the event but stayed within the view of the MRR for the duration (Fig. 7c) and provided a relatively large number of samples. If a free-falling velocity (at 10°C) is assumed, during the initial stages of the event—based on the work by Gat et al. (2001) and Bolin (1958) (and using the equations in Table 3)—only droplets with diameter less than approximately 1 mm would achieve $1/e$ of the final equilibrium state with a relaxation height of approximately 1600 m (estimated using the BB height); while at the end of the event, this would be achieved by all droplets up to approximately 1.25-mm diameter (over the relaxation distance of approximately 2500 m). Therefore, an increase in relaxation distance of nearly 1 km may have contributed to the change in isotopic ratio from the lowest value near the beginning of the event (if the first slightly higher value is assumed to be a consequence of high initial evaporation of descending raindrops in the unsaturated atmosphere) from −87.0‰ to the final value of −31.6‰—a change of 55.4‰, or approximately $+0.055‰\,m^{-1}$ below the melting layer.

However, the number and volume of droplets above the relaxation height–droplet size threshold must be

taken into account as this could help provide insights into the cloud-level isotopic composition. For example, during the initial stages, up to 10% of the droplets (by volume) were calculated to lie outside this theoretical critical size threshold (1 mm), compared to just over 0.1% during the end stages of the event (1.25-mm critical size threshold); therefore, a larger volume of droplets retained the in-cloud isotopic composition during the initial stages of the event because of larger droplets and low melting-level height (thus, shorter relaxation distance).

To fully verify such a hypothesis, further observations would be required. Indeed, if simultaneous samples of cloud water and rainwater isotopic composition were collected in future work, along with MRR observations over an extended height range (e.g., up to 6000 m) and more detailed meteorological information, the development of a model for estimating the vertical variation in rainwater isotopes from ground to cloud level, based on ground-level rainwater composition (in addition to other fractionation processes), could be explored and potentially used to estimate the final equilibrium state.

Nevertheless, the current work does support previous findings. For example, Srivastava et al. (2012) conducted measurements of DSD and stable isotopes in rainwater collected at short intervals (<1 h) in Gadanki, India. The results indicated that evaporation of rain drops at cloud base was insignificant, but a significant negative correlation was observed between $\delta^{18}O$ and droplet size when isotopic variability was large during the rain event (>2‰), indicating that isotopic fractionation by condensation is stronger in rainfall with larger droplets that retain the within-cloud composition (particularly associated with convective rainfall) while less modified (heavier) values occur in rainfall with smaller droplets (larger surface-to-volume ratio). This work and the results presented here suggest that considering DSD could indeed help to improve microphysical models.

Here we show evidence of an amount effect occurring at short time scales (inverse relationship between R and δD; Fig. 8b), made visible and explained using data from the MRR. The depletion of heavy isotopes with increasing amounts of rainfall within individual events can be explained by the preferential isotopic exchange of smaller droplets, which are higher in low-intensity rainfall and drizzle, with near-surface moisture. Therefore, highly fractionated values in intense precipitation are physically related to low rainwater equilibration due to large droplets. In addition, larger raindrops are more depleted in heavy isotopes than smaller ones because of smaller raindrops being formed at an earlier stage in a lower part of the cloud with higher delta values; such drops leave the cloud while the rest remain ascending, growing to larger sizes and becoming isotopically lighter (Miyake et al. 1968). The effect of evaporation on smaller rain drops is also more significant. Different size raindrops represent equilibration with lower or higher levels in the cloud (Gat et al. 2001). As the raindrop falls beneath the cloud, where the air is unsaturated, evaporation occurs, resulting in further enrichment in heavy isotopes. The degree of this enrichment is a function of drop size and therefore rainfall intensity—isotopic equilibration is more complete for less intense rain.

4. Conclusions and recommendations

In contrast to previous studies of controls on water stable isotopic composition focusing on synoptic–seasonal time scales, here we focused on single events at a mid-latitude site. The use of MRR provided an opportunity to thoroughly observe any relationship between stable isotopes and R. We observed a finescale, intra-event amount effect, or local rain intensity effect, occurring within a number of the sample precipitation events.

Despite similar-source air masses, different events can have very different isotopic compositions and isotopic trends. Intra-event trends are linked to local, microphysical, mesoscale, regional, and synoptic signatures (Figs. 1, 5); air mass, rain intensity, rain production altitude, type of precipitation (convective or stratiform), precipitation life cycle and rain-out history, large-scale dynamics, and processes and conditions within the cloud (e.g., drop size, melting layer height, and cloud-base/-top height) and below the cloud (e.g., drop size, temperature, and saturation of the air) all contribute to isotopic fractionation and therefore have an impact on the final isotopic composition of precipitation at any time. The local rain intensity does appear to have an important impact on the changing isotopic composition of rainwater within certain events, while for others there is no apparent relationship.

A full, predictive understanding of the causes of variability requires a combination of more numerous observational campaigns and modeling studies [e.g., Isotope-Incorporated Global Spectral Model (IsoGSM; Yoshimura et al. 2008); amount effect model (Lee and Fung 2008); Community Atmosphere Model, version 3 (CAM3; Barras and Simmonds 2009); Consortium for Small-Scale Modelling Isotope model ($COSMO_{iso}$; Pfahl et al. 2012); 2D column models (Rozanski and Sonntag 1982; Gedzelman and Arnold 1994); and mesoscale convective system model (Kurita 2013)]. This paper has focused on observational data of a type that would be needed to initialize or validate high-temporal- and high-spatial-resolution models. Intra-event sampling campaigns should ideally occur both at ground level and up to cloud level [e.g., using unmanned aerial vehicles (UAVs),

weather balloons to collect data, and cloud water samples at various heights] and at various geographical locations and during the same storm/frontal event (e.g., Coplen et al. 2008), with samples analyzed for both $\delta^{18}O$ and δD (to assess kinetic evaporation). These data should be linked to geophysical data from MRRs, radar, and upper-level soundings to provide a more complete picture of conditions throughout the atmosphere, as well as data and models exploring the larger-scale dynamics and the history of the precipitating system. Technological development in isotopic analysis would now also permit real-time, semicontinuous analyses.

Nevertheless, this study and others (e.g., Celle-Jeanton et al. 2004), have shown how even low-cost measurement techniques can be used to explore intra-event variations. By utilizing an MRR to provide insights into short-term precipitation characteristics, it has highlighted that intra-event isotopic variations in midlatitude rainfall should not be ignored or underestimated, particularly in a changing climate that is expected to result in more extreme precipitation regimes (Allen et al. 2012). Indeed, with inevitable advances in technology, a better understanding of intra-event trends will undoubtedly be achieved in the near future, with potential scientific applications in hydrometeorology (e.g., evaluating GCMs and regional-scale models and predicting intra-event isotopic trends) and hydrology (e.g., understanding vadose and groundwater isotopic composition), as well other fields that could benefit from a more detailed understanding of rainwater isotope variability. There may even be beneficial paleoclimate applications if such information can be utilized in conjunction with work exploring ancient raindrop sizes (e.g., Som et al. 2012).

Acknowledgments. Catherine Muller would like to thank the University of Birmingham for financial support during this research. Andy Baker was supported by a Phillip Leverhulme Prize. We thank Anne Ankcorn for her assistance with sketching the schematic diagram in Fig. 1 and Guillaume Bertrand and the two other anonymous reviewers for their comments, which have been incorporated within this manuscript.

REFERENCES

Adar, E. M., A. Karnieli, B. Z. Sandler, A. Issar, M. Wolf, and L. Landsman, 1991: A mechanical sequential rain sampler for isotopic and chemical analyses. Final Scientific Rep., Contract 5542/RO/Rb, IAEA, Vienna, Austria, 32 pp.

Allen, S. K., and Coauthors, 2012: Summary for policymakers. *Managing the Risks of Extreme Events and Disasters to Advance Climate Change Adaptation,* C. B. Field et al., Eds., Cambridge University Press, 1–19.

Baldini, L. M., F. McDermott, A. M. Foley, and J. U. L. Baldini, 2008: Spatial variability in the European winter precipitation $\delta^{18}O$–NAO relationship: Implications for reconstructing NAO-mode climate variability in the Holocene. *Geophys. Res. Lett.,* **35,** L04709, doi:10.1029/2007GL032027.

——, ——, J. U. L. Baldini, M. J. Fischer, and M. Molloff, 2010: An investigation of the controls on Irish precipitation $\delta^{18}O$ values on monthly and event timescales. *Climate Dyn.,* **35,** 977–993, doi:10.1007/s00382-010-0774-6.

Barras, V., and I. Simmonds, 2009: Observation and modeling of stable water isotopes as diagnostics of rainfall dynamics over southeastern Australia. *J. Geophys. Res.,* **114,** D23308, doi:10.1029/2009JD012132.

Berkelhammer, M., L. Stott, K. Yoshimura, K. Johnson, and A. Sinha, 2012: Synoptic and mesoscale controls on the isotopic composition of precipitation in the western United States. *Climate Dyn.,* **38,** 433–454, doi:10.1007/s00382-011-1262-3.

Bolin, B., 1958: On the uses of tritium as a tracer for water in nature. *Proceedings of the Second UN Conference on the Peaceful Uses of Atomic Energy,* Vol. 18, IAEA, 336– 343.

Celle-Jeanton, H., R. Gonfiantini, Y. Travi, and B. Sol, 2004: Oxygen-18 variations of rainwater during precipitation: Application of the Rayleigh model to selected rainfalls in southern France. *J. Hydrol.,* **289,** 165–177, doi:10.1016/j.jhydrol.2003.11.017.

Coplen, T. B., A. L. Herczeg, and C. Barnes, 2000: Isotope engineering: Using stable isotopes of the water molecule to solve practical problems. *Environmental Tracers in Subsurface Hydrology,* P. G. Cook and A. I. Herczeg, Eds., Kluwer Academic, 529 pp.

——, P. J. Neiman, A. B. White, J. M. Landwehr, F. M. Ralph, and M. D. Dettinger, 2008: Extreme changes in stable hydrogen isotopes and precipitation characteristics in a landfalling Pacific storm. *Geophys. Res. Lett.,* **35,** L21808, doi:10.1029/2008GL035481.

Crawford, J., C. E. Hughes, and S. D. Parkes, 2013: Is the isotopic composition of event based precipitation driven by moisture source or synoptic scale weather in the Sydney basin, Australia? *J. Hydrol.,* **507,** 213–226, doi:10.1016/j.jhydrol.2013.10.031.

Dansgaard, W., 1964: Stable isotopes in precipitation. *Tellus,* **16,** 436–468, doi:10.1111/j.2153-3490.1964.tb00181.x.

Diederich, M., S. Crewell, C. Simmer, and R. Uijlenhoet, 2004: Investigation of rainfall microstructure and variability using vertically pointing radar and disdrometer. *Proc. ERAD 2004,* Visby, Sweden, SMHI, 80–86.

Draxler, R. R., and G. D. Rolph, 2003: HYSPLIT—Hybrid Single Particle Lagrangian Integrated Trajectory Model. NOAA Air Resources Laboratory, Silver Spring, MD. [Available online at www.arl.noaa.gov/ready/hysplit4.html.]

Fairchild, I. J., and A. Baker, 2012: *Speleothem Science: From Process to Past Environments.* Wiley, 450 pp.

Field, R. D., 2010: Observed and modeled controls on precipitation $\delta^{18}O$ over Europe: From local temperature to the northern annular mode. *J. Geophys. Res.,* **115,** D12101, doi:10.1029/2009JD013370.

Friedman, I., L. Machta, and R. Soller, 1962: Water vapour exchange between a water droplet and its environment. *J. Geophys. Res.,* **67,** 2761–2766, doi:10.1029/JZ067i007p02761.

Gat, J. R., W. G. Mook, and H. A. J. Meijer, 2001: *Atmospheric Water.* Vol. 2, *Environmental Isotopes in the Hydrological Cycle,* UNESCO/IAEA, 235 pp.

Gedzelman, S. D., and J. R. Lawrence, 1990: The isotopic composition of precipitation from two extratropical cyclones. *Mon. Wea. Rev.,* **118,** 495–509, doi:10.1175/1520-0493(1990)118<0495:TICOPF>2.0.CO;2.

——, and R. Arnold, 1994: Modeling the isotopic composition of precipitation. *J. Geophys. Res.,* **99,** 10 455–10 472, doi:10.1029/93JD03518.

Gonfiantini, R., M.-A. Roche, J.-C. Olivry, J.-C. Fontes, and G. M. Zuppi, 2001: The altitude effect on the isotopic composition of tropical rains. *Chem. Geol.,* **181,** 147–167, doi:10.1016/S0009-2541(01)00279-0.

Guglielmo, F., and Coauthors, 2013: Using water isotopes in the evaluation of land surface models. *Geophysical Research Abstracts,* Vol. 15, Abstract EGU2013-11436-1. [Available online at http://meetingorganizer.copernicus.org/EGU2013/EGU2013-11436-1.pdf.]

Helsen, M. M., R. S. W. van de Wal, M. R. van den Broeke, D. van As, H. A. J. Meijer, and C. H. Reijmer, 2005: Oxygen isotope variability in snow from western Dronning Maud Land, Antarctica and its relation to temperature. *Tellus,* **57B,** 423–435, doi:10.1111/j.1600-0889.2005.00162.x.

Hoefs, J., 1997: *Stable Isotope Geochemistry*. 4th ed. Springer-Verlag, 201 pp.

Houze, R. A., Jr., 1993: *Cloud Dynamics*. Academic, 573 pp.

Jouzel, J., 1986: Isotopes in cloud physics: Multiphase and multistage condensation process. *Handbook of Environmental Isotope Geochemistry,* Vol. 2, P. Fritz and J. Ch. Fontes, Eds., Elsevier Science, 61–112.

Kurita, N., 2013: Water isotopic variability in response to mesoscale convective system over the tropical ocean. *J. Geophys. Res. Atmos.,* **118,** 10 376–10 390, doi:10.1002/jgrd.50754.

——, K. Ichiyanagi, J. Matsumoto, M. D. Yamanaka, and T. Ohata, 2009: The relationship between the isotopic content of precipitation and the precipitation amount in tropical regions. *J. Geochem. Explor.,* **102,** 113–122, doi:10.1016/j.gexplo.2009.03.002.

Lai, C. T., J. R. Ehleringer, B. J. Bond, and U. K. T. Paw, 2006: Contributions of evaporation, isotopic non-steady state transpiration and atmospheric mixing on the $\delta^{18}O$ of water vapour in Pacific Northwest coniferous forests. *Plant Cell Environ.,* **29,** 77–94, doi:10.1111/j.1365-3040.2005.01402.x.

Lawrence, J. R., S. D. Gedzelman, J. W. C. White, D. Smiley, and P. Lazov, 1982: Storm trajectories in eastern US D/H isotopic composition of precipitation. *Nature,* **296,** 638–640, doi:10.1038/296638a0.

Lee, J., and I. Fung, 2008: ''Amount effect'' of water isotopes and quantitative analysis of post-condensation processes. *Hydrol. Processes,* **22,** 1–8, doi:10.1002/hyp.6637.

Levin, M., J. R. Gat, and S. A. Issar, 1980: Precipitation, flood and groundwater of the Negev Highlands: An isotopic study of desert hydrology. *Arid-Zone Hydrology: Investigations with Isotope Techniques,* IAEA, 3–22.

Mason, B. J., and R. Ramanadham, 1954: Modification of the size distribution of falling raindrops by coalescence. *Quart. J. Roy. Meteor. Soc.,* **80,** 388–394, doi:10.1002/qj.49708034508.

Miyake, Y., O. Matsubaya, and C. Nishihara, 1968: An isotopic study on meteoric precipitation. *Pap. Meteor. Geophys.,* **19,** 243–266.

Morrison, J., T. Brockwell, F. F. Merren, and A. M. Phillips, 2001: On-line high-precision stable hydrogen isotopic analyses on nanoliter water samples. *Anal. Chem.,* **73,** 3570–3575, doi:10.1021/ac001447t.

Muller, C. L., A. Baker, R. Hutchinson, I. J. Fairchild, and C. Kidd, 2008: Analysis of rainwater dissolved organic carbon compounds using fluorescence spectrophotometry. *Atmos. Environ.,* **42,** 8036–8045, doi:10.1016/j.atmosenv.2008.06.042.

——, C. Kidd, I. J. Fairchild, and A. Baker, 2010: Investigation into clouds and precipitation over an urban area using micro rain radars, satellite remote sensing and fluorescence spectrophotometry. *Atmos. Res.,* **96,** 241–255, doi:10.1016/j.atmosres.2009.08.003.

Munksgaard, N. C., C. M. Wurster, A. Bass, and M. I. Bird, 2012: Extreme short-term stable isotope variability revealed by continuous rainwater analysis. *Hydrol. Processes,* **26,** 3630–3634, doi:10.1002/hyp.9505.

Pfahl, S., H. Wernli, and K. Yoshimura, 2012: The isotopic composition of precipitation from a winter storm—A case study with the limited-area model $COSMO_{iso}$. *Atmos. Chem. Phys.,* **12,** 1629–1648, doi:10.5194/acp-12-1629-2012.

Poage, M. A., and C. P. Chamberlain, 2001: Empirical relationships between elevation and the stable isotope composition of precipitation and surface waters: Considerations for studies of paleoelevation change. *Amer. J. Sci.,* **301,** 1–15, doi:10.2475/ajs.301.1.1.

Rindsberger, M., S. Jaffe, S. Rahamim, and J. R. Gat, 1990: Patterns of the isotopic composition of precipitation in time and space: Data from the Israeli storm water collection program. *Tellus,* **42B,** 263–271, doi:10.1034/j.1600-0889.1990.t01-2-00005.x.

Risi, C., S. Bony, and F. Vimeux, 2008a: Influence of convective processes on the isotopic composition ($\delta^{18}O$ and δD) of precipitation and water vapor in the tropics: 2. Physical interpretation of the amount effect. *J. Geophys. Res.,* **113,** D19306, doi:10.1029/2008JD009943.

——, ——, ——, L. Descroix, B. Ibrahim, E. Lebreton, I. Mamadou, and B. Sultan, 2008b: What controls the isotopic composition of the African monsoon precipitation? Insights from event-based precipitation collected during the 2006 AMMA field campaign. *Geophys. Res. Lett.,* **35,** L24808, doi:10.1029/2008GL035920.

——, and Coauthors, 2012: Process-evaluation of tropospheric humidity simulated by general circulation models using water vapor isotopologues: 1. Comparison between models and observations. *J. Geophys. Res.,* **117,** D05303, doi:10.1029/2011JD016621.

——, A. Landais, R. Winkler, and F. Vimeux, 2013: Can we determine what controls the spatio–temporal distribution of d-excess and ^{17}O-excess in precipitation using the LMDZ general circulation model? *Climate Past,* **9,** 2173–2193, doi:10.5194/cp-9-2173-2013.

Rozanski, K., and C. Sonntag, 1982: Vertical distribution of deuterium in atmospheric water vapour. *Tellus,* **34A,** 135–141, doi:10.1111/j.2153-3490.1982.tb01800.x.

——, L. Araguás-Araguás, and R. Gonfiantini, 1993: Isotopic patterns in modern global precipitation. *Climate Change in Continental Isotopic Records, Geophys. Monogr.,* Vol. 78, Amer. Geophys. Union, 1–36, doi:10.1029/GM078p0001.

Smith, R. B., 1992: Deuterium in North Atlantic storm tops. *J. Atmos. Sci.,* **49,** 2041–2057, doi:10.1175/1520-0469(1992)049<2041:DINAST>2.0.CO;2.

Sodemann, H., 2006: Tropospheric transport of water vapour: Lagrangian and Eulerian perspectives. Ph.D. dissertation 16623, ETH Zurich, 245 pp. [Available online at http://e-collection.library.ethz.ch/eserv/eth:28833/eth-28833-02.pdf.]

Som, S. M., D. C. Catling, J. P. Hammeijer, P. M. Polivka, and R. Buick, 2012: Air density 2.7 billion years ago limited to less than twice modern levels by fossil raindrop imprints. *Nature,* **484,** 359–362, doi:10.1038/nature10890.

Srivastava, R., R. Ramesh, and T. Narayana Rao, 2012: Relationship between stable isotope ratios and drop size distribution in tropical rainfall. *J. Atmos. Chem.,* **69,** 23–31, doi:10.1007/s10874-012-9227-4.

Strong, M., Z. D. Sharp, and D. S. Gutzler, 2007: Diagnosing moisture transport using D/H ratios of water vapour. *Geophys. Res. Lett.,* **34,** L03404, doi:10.1029/2006GL028307.

Sturm, C., Q. Zhang, and D. Noone, 2010: An introduction to stable water isotopes in climate models: Benefits of forward proxy modelling for paleoclimatology. *Climate Past,* **6,** 115–129, doi:10.5194/cp-6-115-2010.

Taupin, J.-D., and R. Gallaire, 1998: Isotopic variability in some intra-storm in the region of Niamey, Niger. *C. R. Acad. Sci., Ser. IIa,* **326,** 493–498.

Treble, P., W. F. Budd, P. K. Hope, and P. K. Rustomji, 2005: Synoptic scale climate patterns associated with rainfall $\delta^{18}O$ in southern Australia. *J. Hydrol.,* **302,** 270–282, doi:10.1016/j.jhydrol.2004.07.003.

Vimeux, F., R. Gallaire, S. Bony, G. Hoffmann, and J. C. H. Chiang, 2005: What are the climate controls on δD in precipitation in the Zongo Valley (Bolivia)? Implications for the Illimani ice core interpretation. *Earth Planet. Sci. Lett.,* **240,** 205–220, doi:10.1016/j.epsl.2005.09.031.

Yoshimura, K., M. Kanamitsu, D. Noone, and T. Oki, 2008: Historical isotope simulation using reanalysis atmospheric data. *J. Geophys. Res.,* **113,** D19108, doi:10.1029/2008JD010074.

——, ——, and M. Dettinger, 2010: Regional downscaling for stable water isotopes: A case study of an atmospheric river event. *J. Geophys. Res.,* **115,** D18114, doi:10.1029/2010JD014032.

Yurtsever, Y., and J. R. Gat, 1981: Atmospheric waters. *Stable Isotope Hydrology: Deuterium and Oxygen-18 in the Water Cycle,* J. R. Gat and R. Gonfiantini, Eds., Tech. Rep. 2010, IAEA, 103–142.